Available online at www.sciencedirect.com
SCIENCE DIRECT®
Microporous and Mesoporous Materials 83 (2005) 25–34
MICROPOROUS AND MESOPOROUS MATERIALS
www.elsevier.com/locate/micromeso

Characterisation of the acid–base properties of pillared montmorillonites

Manju Kurian, S. Sugunan *

Department of Applied Chemistry, Cochin University of Science and Technology, Kochi 682 022, India

Received 6 November 2004; received in revised form 26 February 2005; accepted 10 March 2005
Available online 23 May 2005

Abstract

Iron and mixed iron aluminium pillared montmorillonites prepared by partial hydrolysis method were subjected to room temperature exchange with transition metals of the first series. The resulting materials were characterised by different spectroscopic techniques and surface area measurements. About 1–3% transition metals were incorporated into the porous network. The structural stability of the porous network was not affected by exchange. XRD and ^{27}Al NMR spectroscopy evidenced the presence of iron substituted Al_{13} like polymers in FeAl pillared systems. Acidity and basicity benefited much as a result of metal exchange. Acidity and basicity were quantified by model reactions, viz., cumene cracking and cyclohexanol decomposition respectively. The presence of basic sites in otherwise acidic pillared clays, though diminutive in amount can be of much importance in acid base catalysed reactions.

Keywords: Catalysis; Pillared clays; Surface acidity; Cumene cracking; Surface basicity; Cyclohexanol decomposition

1. Introduction

Pillaring of smectites with robust, polynuclear inorganic cations remains a lively research area. These modified clay minerals have attracted considerable attraction as acid catalysts for petroleum refining [1] and other acid catalysed reactions [2–4]. Iron oligomers are one of the most widely used pillaring agent because iron pillared clays are cheaper to prepare and would not only have acidic properties but also contain pillars that in themselves would be catalytically active and have redox and magnetic properties [5].

The acid structure of the pillared clays has been well characterised by different probe molecules and using different methods [6,7]. However, the basic sites though expected to a limited extent, have not been characterised well. The qualification of the basic sites as well as their quantification will help in the potential use of these materials in acid base catalysed reactions. Alcohol decomposition has been widely studied because it is a simple model reaction to determine the functionality of a catalyst. Cyclohexanol undergoes dehydration over acidic sites giving cyclohexene as the major product whereas a combination of acidic and basic sites is required for the dehydrogenation yielding cyclohexanone. Cyclohexene on disproportionation yields benzene, cyclohexane and methylcyclopentane [8]. Thus, product selectivity gives a quantitative estimate of surface acid base properties. Moreover, cyclohexanone is the key intermediate for the manufacture of Nylon 6, Nylon 6,6 for synthetic fibre and tire cord [9]. Present industrial practice of cyclohexanone production involves catalytic dehydrogenation of cyclohexanol over commercial grade copper oxide supported on zinc oxide (Girdler-G-66B) [10].

* Corresponding author. Tel.: +91 484 2575804; fax: +91 484 2577595.
E-mail address: ssg@cusat.ac.in (S. Sugunan).

1387-1811/$ - see front matter © 2005 Elsevier Inc. All rights reserved.
doi:10.1016/j.micromeso.2005.03.001

In this paper, we report the activities of transition metal exchanged iron and iron aluminium mixed pillared systems for the decomposition of cyclohexanol. To our knowledge, not many reports have appeared in the characterisation of basic sites of pillared clays. The effects of reaction variables on cyclohexanol decomposition have been studied well. The prepared materials have been characterised by different spectroscopic techniques as well as surface area and pore volume measurements.

2. Materials and methods

The pillaring species was synthesised by partial hydrolysis of 0.1 M $Fe(NO_3)_3$ solution by drop wise addition of 0.3 M Na_2CO_3 solution under vigorous stirring (for iron aluminium mixed pillaring, equimolar ratios of $Fe(NO_3)_3$ and $Al(NO_3)_3$ were taken). N_2 gas was bubbled through the solution to remove excess CO_2 and aged for 24 h at room temperature. Intercalation of pillaring species into the clay layers was done by treating the pillaring solution with a previously swollen clay suspension at 80 °C [OH/metal ratio, 2 and metal/clay ratio, 20 mmol/g clay]. The clay after exchange was washed several times with distilled water and filtered. This was dried in air oven at 110 °C overnight, followed by calcination for 6 h at 450 °C in muffle furnace. Exchange with transition metals was done using 0.1 molar aqueous solutions of the corresponding metal nitrate. For exchange with vanadium, requisite amount of ammonium metavanadate was dissolved in oxalic acid. Pillared clays were stirred mechanically with salt solutions for 24 h at room temperature. The clay after exchange was washed 5–6 times with distilled water. This was filtered and dried in air oven at 110 °C overnight and calcined for 5 h at 500 °C. The pillared clays synthesised for the present study are notated as X/Fe PM or X/FeAl PM where X is the transition metal exchanged.

EDX analysis of the prepared samples was done in a JEOL JSM-840 A (Oxford make model 16211 with a resolution of 1.3 eV). The diffractometer traces were taken in RIGAKU D/MAX-C instrument using Cu Kα radiation (λ = 1.5405 Å). The simultaneous determination of surface area and pore volumes of the samples were done on a Micromeritics Gemini analyser. Previously activated samples were degassed at 200 °C under nitrogen atmosphere for 2 h and then brought to nitrogen boiling point. FTIR spectra were recorded using a Perkin Elmer RX-1 spectrometer by the KBr disc method in the range 400–4000 cm^{-1}. NMR spectra of samples were recorded by a 300 DSX Brucker spectrometer. Shimadzu TGA-50 instrument was used for thermogravimetric studies. About 10 mg of the sample was used at a heating rate of 20 °C per minute in the temperature range of 50–600 °C. UV-DRS spectra of the samples were taken in an Ocean Optics instrument using MgO as the reference material.

The test reactions for acidity and basicity were carried out at atmospheric pressure in a fixed bed, downflow vertical glass reactor (1 cm diameter, 40 cm length) inside a double zone furnace. 0.5 g catalyst activated at 500 °C was immobilised inside the reactor using glass wool, sandwiched between inert silica beads. A thermocouple positioned near the catalyst bed monitored the reaction temperature, regulated using a temperature controller. Cyclohexanol or cumene were fed into the reactor with the help of a syringe pump at controlled flow rate. The products were collected downstream the reactor in a receiver connected through a water condenser and analysed using Chemito 8610 Gas Chromatograph equipped with Flame Ionisation Detector and appropriate column.

3. Results and discussion

3.1. Energy dispersive X-ray analysis

The elemental compositions of the individual systems as obtained from EDX are presented in Table 1. The parent clay has considerable amount of exchangeable cations, viz., Na, Mg, K and Ca. A drastic reduction in the amount of these elements occurs on pillaring with iron and for Fe PM the amount of iron increases by 23.54%. Increase in iron content with corresponding decrease in the amount of exchangeable cations points to successive replacement of interlamellar cations with stable iron oxide pillars. Insertion of oligomeric species occurs at the expense of exchangeable cations as indicated by marked decrease in the amount of Na, K, Mg and Ca. For FeAl PM, Fe and Al content of pillared system increases from the original clay by 5.62% and 3.67%. Room temperature exchange with transition metals incorporates about 1–3% of the metals into the pillared system. Vanadium and zinc exchange best with single pillared systems while zinc and manganese is loaded to greater extent in the mixed pillared series.

In order to show the effects of exchange process on the original constituents of the clay, the elemental weights can be recalculated to 100% after excluding the fixed transition metal oxide. This calculation indicates that transition metal oxide was introduced without a significant deleterious effect on the clay structure and the pillars. Thus on exchange with transition metal, metal oxides are incorporated into the pores or in between the pillars rather than exchanged in the location of pillars.

3.2. Surface area and pore volume measurements

The determination of surface area and pore volume in clays is a subject of controversy. The surface areas of pil-

Table 1
Elemental composition of the systems

Catalyst	Element (%)[a]							
	Na	Mg	Al	Si	K	Ca	Fe	TM[b]
V/Fe PM	0.29	1.38	14.09	46.96	1.11	0.41	33.43	2.33
Mn/Fe PM	0.31	1.52	14.71	46.85	1.07	0.44	35.1	1.19
Co/Fe PM	0.37	1.34	14.09	46.52	1.85	0.50	33.36	1.97
Ni/Fe PM	0.44	1.85	14.78	47.06	1.54	0.49	33.84	1.93
Cu/Fe PM	0.36	1.03	14.46	47.94	1.61	0.42	32.97	1.21
Zn/Fe PM	0.34	1.84	14.12	47.12	1.64	0.46	31.22	2.26
Fe PM	0.33	1.42	14.88	45.55	1.91	0.56	35.21	0
V/FeAl PM	0.23	1.48	20.69	56.18	1.8	0.35	17.08	1.99
Mn/FeAl PM	0.21	1.58	19.95	56.07	2.19	0.39	16.9	2.51
Co/FeAl PM	0.22	1.59	21.29	56.0	2.02	0.41	17.01	1.26
Ni/FeAl PM	0.28	1.78	21.22	56.26	2.04	0.4	17.02	1.3
Cu/FeAl PM	0.32	1.46	20.73	55.85	2.24	0.31	17.29	1.8
Zn/FeAl PM	0.22	1.83	19.94	55.0	1.57	0.43	16.73	3.18
FeAl PM	0.31	1.97	21.41	56.61	2.67	0.54	17.29	0
M	2.18	2.81	17.74	56.47	4.11	5.01	11.67	0

[a] As determined by energy dispersive X-ray analysis. The reported values are within the error limit of ±5%.
[b] Exchanged transition metal.

lared clays are typically obtained by applying BET equation to the N_2 adsorption isotherm. The range of validity of BET equation for these materials is usually between $P/P_0 = 0.01$ and 0.1. However, in microporous solids like pillared clays where the interlamellar distance is of the order of a few molecular diameters, monolayer formation on clay silicate layers occurs. Thus surface areas approximated by Langmuir equation are reasonable representations of pillared clay surface areas. Hence in the present study, BET and Langmuir surface areas of various systems obtained directly are tabulated.

The surface areas and pore volumes of the prepared systems are given in Table 2. Montmorillonite has a BET surface area of 14.3 $m^2 g^{-1}$ and Langmuir surface area of 27.9 $m^2 g^{-1}$. As a result of pillaring, surface area and pore volume increases substantially, this effect being maximum for iron pillaring. Transition metal exchange decreases the surface area and pore volume. The external surface area in pillared clays arises from mesopores which are mainly interparticle voids. Transition metal exchange deposits the metal oxides inside the porous network and hence the decrease in surface area and pore volume. Minimum surface area is exhibited by zinc exchanged system. Decrease in surface area can be roughly correlated to the amount of metal oxide incorporated as obtained from EDX measurements.

Table 2
Surface area and pore volume of the systems

Catalyst	Surface area ($m^2 g^{-1}$)		Pore volume[a] (ccg^{-1})
	BET	Langmuir	
V/Fe PM	160	234	0.20
Mn/Fe PM	194	285	0.21
Co/Fe PM	178	251	0.19
Ni/Fe PM	165	227	0.19
Cu/Fe PM	171	248.2	0.20
Zn/Fe PM	148	235	0.18
Fe PM	194	270	0.21
V/FeAl PM	158	230	0.17
Mn/FeAl PM	156	219	0.17
Co/FeAl PM	164	229	0.19
Ni/FeAl PM	142	204	0.17
Cu/FeAl PM	144	207	0.16
Zn/FeAl PM	147	233	0.16
FeAl PM	170	253	0.19
M[b]	14	27	0.005

[a] Pore volume measured at $0.9976P/P_0$.
[b] Montmorillonite KSF.

3.3. X-ray diffraction

Excepting surface area and pore volume measurements, the easiest way to determine whether pillar intercalation is successful is to record the X-ray diffraction pattern of an oriented film of the product. Pillared clays are semi crystalline in nature. The broad bands obtained in the XRD spectrum, instead of sharp peaks can be attributed to semi crystalline nature of clays (Fig. 1). X-ray profile indicates that long range face to face layer aggregation is present in the pillared sample. Thus, it can be safely commented that the sample is not an edge to face delaminated clay.

The characteristic d_{001} spacing of montmorillonite increased from 9.8 Å to 19.2 Å and 17.8 Å for Fe PM and FeAl PM respectively. Shifting of 2θ values clearly suggest expansion of clay layer during pillaring process. Bergaya et al. reported the formation of mixed Al_{13-x}-Fe_x pillars, based on the Fe content of the pillared solids [11]. The d spacing of (001) plane increased from 9.8 Å to 17.8 Å in the present case indicating the presence of iron substituted Al_{13} like polymers. This polymer with structural formula, $[AlO_4Al_{12}(OH)_{24}(H_2O)_{12}]^{7+}$ is a

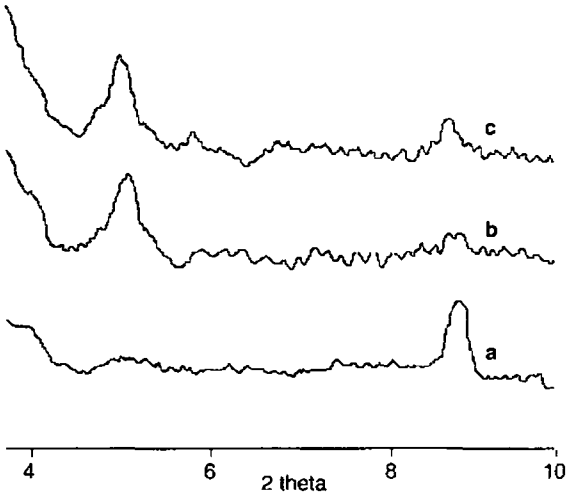

Fig. 1. XRD profile: (a) M, (b) Fe PM, and (c) FeAl PM.

tri-decamer composed of one aluminium tetrahedra surrounded by 12 aluminium octahedra. It contains four layers of superimposed oxygen atoms needed for expanding clay basal spacings to 18 Å.

The XRD patterns of the metal exchanged systems were exactly identical to that of the parent pillared clay. Additional peaks corresponding to the exchanged metal oxides were not noticed. This may be due to the diminutive amounts (1–3%) of the exchanged metal in these samples. Thus, insertion of the second metal after the formation of stable pillars does not destabilise the porous network.

3.4. Fourier transform infra red spectroscopy

The structural evolution of the aluminosilicate layer characterised by FTIR spectroscopy is given in Fig. 2. The parent montmorillonite points up a large band at

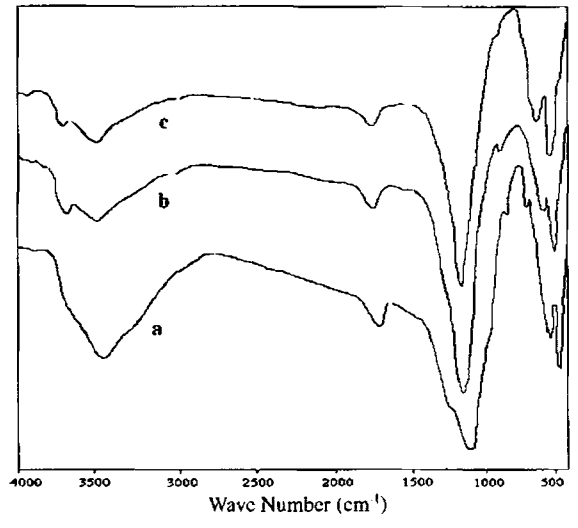

Fig. 2. FTIR spectra: (a) M, (b) Fe PM, and (c) FeAl PM.

3620 cm^{-1}, typical of smectites with large amount of Al in the octahedral [12]. Intensity of this peak decreases upon pillaring. Formation of a new band in the range of 3740–3770 cm^{-1} is an important observation. The identification of hydroxyl species on pillared clays is extremely difficult, because of the complexity of the system and the opaqueness of the sample in the corresponding IR region. It has been reported that isotopic exchange with mild deuterating agent C_6D_6 has allowed identifying two acidic hydroxyls, with OH stretching modes at 3660 and 3740 cm^{-1}, the former referring to the unstructured band of the parent montmorillonite and the latter which seem to arise from the sealing of montmorillonite layer and the pillar. These can be represented as Si–O–Al–OH or Al–O–Si–OH. Thus FTIR spectra also are indicative of effective pillaring.

The IR spectra in the fingerprint region are characterised by absorptions at 1200–1000 cm^{-1} due to asymmetric stretching vibrations of apical oxygens of SiO_2 tetrahedra and the large band due to combined stretching and bending vibrations of the Si–O bonds related to basal oxygens. The band around 900 cm^{-1} often provides information on the composition of octahedral sheets. In montmorillonite, it reflects partial substitution of octahedral Al by Mg. Absorptions at 526–471 cm^{-1} echo bending Si–O vibrations. Thus, the framework vibrations contain information about the structural characteristics of the material and their preservation after thermal treatments may be considered as a proof of the structural stability on pillaring. Absence of additional peaks suggests that no bond formation occurs between montmorillonite and pillars unlike other clays like saponite.

3.5. ^{27}Al nuclear magnetic resonance spectroscopy

Clay minerals and pillared clays have been the subject of several solid state NMR investigations. The ^{27}Al MAS NMR spectra of the pillared clays are illustrated in Fig. 3. Montmorillonite shows two resonances; one at +1.38 ppm that can be ascribed to octahedral Al atoms and other at +66.0 ppm attributable to tetrahedrally coordinated Al atoms. For Fe PM, intensity of ^{27}Al NMR peaks at the octahedral and tetrahedral Al sites are almost similar to that of montmorillonite. Thus, there is non existence of Al atoms in the extra framework region. But the peaks are somewhat broader. This can be due to relaxation effects of paramagnetic centres. The ^{27}Al NMR spectrum for FeAl PM shows the Al^{IV} signature of Keggin cation at +65.8 ppm. Resonance corresponding to octahedral Al atoms also is shifted to +1.97 ppm. Thus the pillaring solution would be made from these cations in which Al^{3+} is partially replaced by Fe^{3+}. The nature of substitution is not known, but in view of Al by Fe in octahedral layers of micas, it is likely that some of the octahedral Al atoms in Keggin

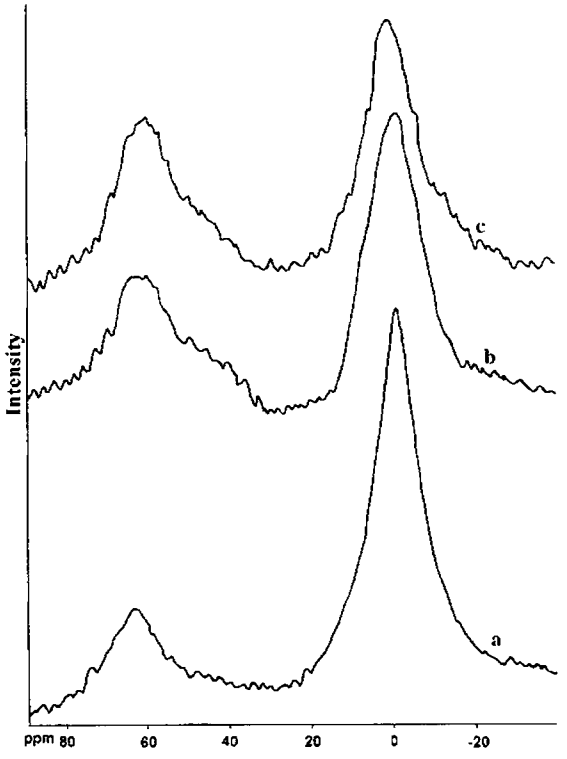

Fig. 3. ^{27}Al NMR spectra: (a) M, (b) Fe PM, and (c) FeAl PM.

structure are replaced by Fe atoms [13]. Here also, relaxation effects caused by paramagnetic centres are operative. Hence FWHM (full width at half maximum) of the peaks is greater, compared to montmorillonite.

The effect of transition metal exchange on structural stability of pillared clays was examined by taking ^{27}Al MAS NMR spectra of copper and cobalt doped iron pillared systems as representative systems. As a result of exchange with transition metals, peak width as well as peak positions do not vary. Thus, incorporation of transition metals does not affect the structural stability of layers and pillars. Hence ^{27}Al NMR data supports the inference drawn from surface area and pore volume measurements, that metal oxides are incorporated into porous network rather than attached to pillars.

3.6. ^{29}Si nuclear magnetic resonance spectroscopy

Fig. 4 illustrates the ^{29}Si MAS NMR spectra of montmorillonite and pillared systems. Montmorillonite shows a single resonance centred on −93 ppm. The peak shows a main peak at −93.98 ppm and two shoulder peaks: a large one at −104.5 ppm and a diminutive one at −90.3 ppm. The peak at −93.98 ppm can be attributed to Q^3 (Si1Al) units representing Si(IV) atoms linked through oxygen atoms to three other Si(IV) and to one Al(VI) (or Mg) in the clay octahedral layer. The shoulder peak at −104.5 ppm can be ascribed to Q^3 (Si0Al) where Si is linked to Si only through oxygen

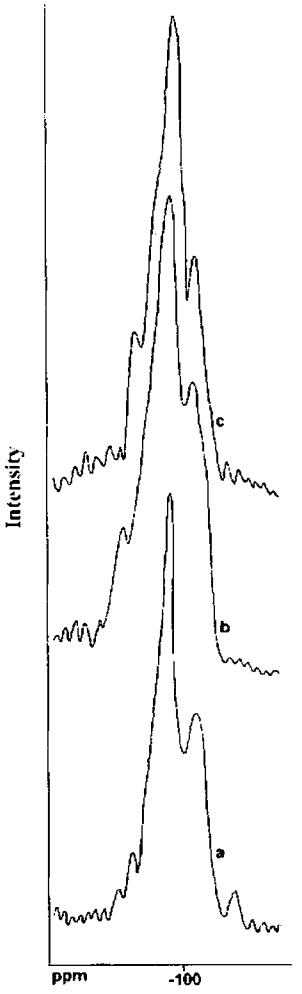

Fig. 4. ^{29}Si NMR spectra: (a) M, (b) Fe PM, and (c) FeAl PM.

and small peak at −90.3 ppm is due to Q^3 (Si2Al). Thus majority of the silicon tetrahedra is linked to 3 Si atoms and one Al atom. A very small portion is linked to 2 Al atoms and 2 Si atoms while a part of Si tetrahedra is linked to Si atoms alone. This distribution of silicon tetrahedra into various environments is not affected by pillaring. A slight shift in ppm values can be noticed for the pillared samples and this is tabulated in Table 3. From the table it can be inferred that Lowenstein rule is obeyed. Lowenstein rule is the avoidance rule, which states that two tetrahedral Al cannot be next neighbours.

Table 3
Distribution of Si atoms to different environments

Catalyst	Q^3 (Si0Al)[a] (ppm)	Q^3 (Si1Al)[a] (ppm)	Q^3 (Si2Al)[a] (ppm)
M[b]	−90.3	−93.98	−104.5
Fe PM	−91.6	−95.6	−105.98
FeAl PM	−91.02	−94.34	−105.35

[a] As determined by ^{29}Si MAS NMR spectroscopy.
[b] Montmorillonite KSF.

Also, the shift in ppm values is in the order Fe PM > FeAl PM. The order is the same as the order of d spacing obtained from X-ray diffraction studies. Thus the shift in ppm, which indicates strain in the local environment of Si atoms, is proportional to size of intercalated species.

Several authors have pointed out that inversion of silicon tetrahedra can occur with intercalation of polymeric species in clays like beidellite and saponite where the layer charge is localised in tetrahedral layer [14,15]. Such an inversion is not anticipated in montmorillonite since the layer charge is not localised. ^{29}Si MAS NMR spectra confirm this point since the shift in δ ppm values is less than 1–2 ppm in all pillared samples. The contributions of different Si environments also remain the same. This gives confirmation to the nonexistence of chemical bonds between exchanged polymeric species and clay layers. Thus as anticipated, pillaring which is only a cation exchange process does not affect the short range order within clay layers. Had any bond that forms Al-O-Si linkage between the pillars and silicate layers been formed, the spectra would have contained Q^3 (Si3Al) resonance.

The effect of exchange with transition metals on the structural stability of clay as well as pillaring process was exposed by taking the ^{29}Si NMR spectra of two of the exchanged systems viz., cobalt and zinc exchanged systems. The peak positions do not alter much as a result of exchange with transition metals. Thus incorporation of transition metals on Fe PM does not alter the local environment of Si atoms. Hence, it can be inferred that metal oxides are not in the immediate environment of Si layer. They may be present in the porous network of the pillared system. This has been evidenced by surface area data and ^{27}Al MAS NMR spectra.

3.7. Thermogravimetric analysis

Lack of thermal stability is the common drawback attributed to pillared clays. In order to find out thermal stability of prepared systems, it was subjected to thermogravimetric analysis in the temperature range of 30–800 °C. TG-DTA profiles (Fig. 5) show that the pillared systems possess substantial thermal stability. Weight loss occurred in two steps for montmorillonite. After losing weight at 100–120 °C, weight of montmorillonite remains almost constant to about 650 °C. Thus, endothermic peaks corresponding to release of water alone, either by simple desorption or by hydroxylation of OH groups are detected. The latter process occurred at high temperature while weight loss at 100–120 °C characterised dehydration of samples. The temperature of dehydroxylation can be related to thermal stability of the pillared sample. Hence the thermal stability of pillared clays is in the order FeAl PM > Fe PM. However,

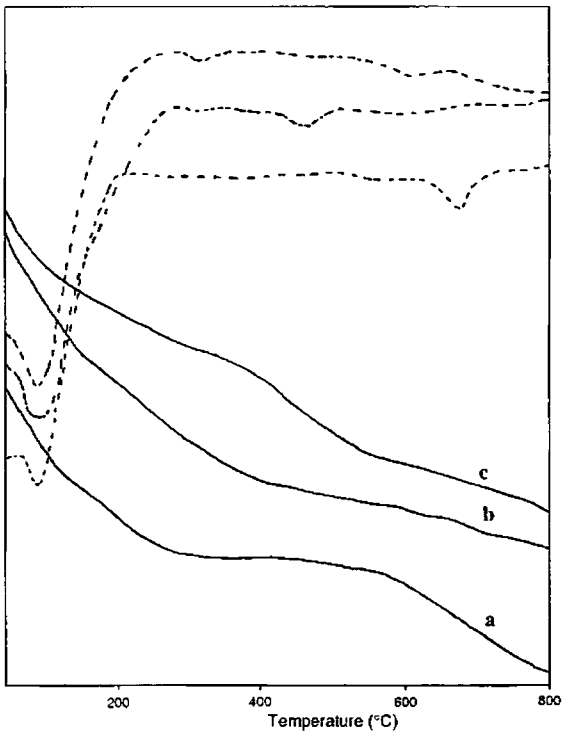

Fig. 5. TG-DTA profile: (a) M, (b) Fe PM, and (c) FeAl PM.

an additional dip around 300 °C was noticed for the pillared systems. For Fe PM, the third weight loss occurred around 500 °C where as for FeAl PM, it was observed in the range of 600 °C. The second dip for iron containing pillars, occurring around 300 °C can be attributed to conversion of oligomeric species to stable iron oxide pillars. Similar observations were reported by Zhao et al. [13]. Dehydroxylation of water associated with lattice Fe^{3+} ions above 720 °C have been reported [16]. However this was not observed in the present study.

3.8. Ultraviolet diffuse reflectance spectroscopy

UV diffuse reflectance spectroscopy has increasingly been applied to investigate structures of solid catalysts due to charge transfer spectra in ultraviolet region. DRS can favourably complement surface studies of transition metal compounds, although it is restricted to information on first shell (metal- oxygen interaction). The UV-DR spectra of montmorillonite and pillared systems are presented in Fig. 6. A band centred at 250–280 nm is present in all systems. This is due to presence of Si in tetrahedral coordination. This band becomes higher for mixed pillared samples due to contribution of tetrahedrally coordinated aluminium in Keggin structure [17]. Thus, UV-DRS also supports the presence of Keggin cation in these systems. The spectra for iron pillared and mixed pillared systems show one band at 300 nm that could be assigned to polyoxo-iron complexes. The hydrolysis reactions of Fe(III) are

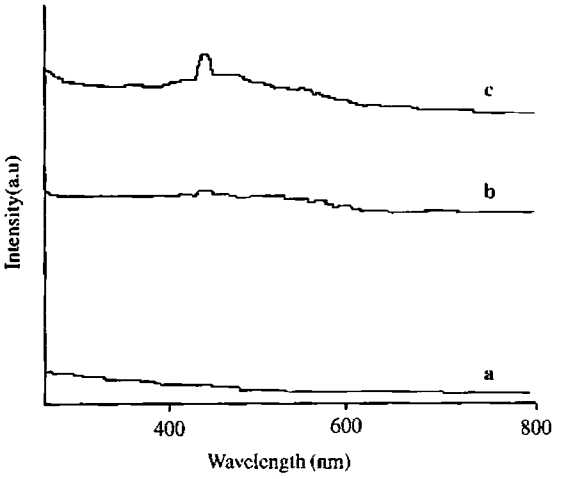

Fig. 6. UV DRS spectra: (a) M, (b) Fe PM, and (c) FeAl PM.

known to yield discrete spherical polycations with an estimated diameter of 15–30 Å. As expected, the intensity of this peak is higher for single oxide system than the mixed pillared system. Exchange with transition metals does not alter the spectra much. Though, bands due to d-d and charge transfer transitions can be expected in metal oxides like vanadium and zinc, they are not observed in the present case. This may be due to low concentration (1–2%) these metals in the systems.

3.9. Surface acidity by cumene cracking test reaction

Cumene is a conventional model compound for testing the catalytic activity since it undergoes diverse reactions over different types of acid sites. Major reactions taking place during cracking of cumene are dealkylation or cracking to benzene and propene and dehydrogenation to α-methyl styrene. Small amounts of ethylbenzene and toluene can be formed by cracking of side chain, which on dehydrogenation gives styrene. Cracking of cumene is generally attributed to Brönsted acid sites by a carbonium ion mechanism. α-Methyl styrene is formed on Lewis acid sites [18].

The catalytic performance of the prepared systems under optimised conditions is given in Table 4. Ethylbenzene and styrene appeared in minor quantities and in some cases toluene also was detected. All the dealkylated products are bannered together and Lewis to Brönsted ratio gives the ratio between the dehydrogenated and cracked products. Iron pillared clay shows very good activity towards the reaction with high selectivity towards α-methyl styrene. Lewis/Brönsted acid ratio is 1.37 for Fe PM. Exchange with transition metals increases the activity except for Co/Fe PM and Zn/Fe PM. It has been documented that catalytic activity for cumene cracking can be correlated to total acidity of the samples. Also, dehydrogenation to α-methyl styrene occurs over Lewis acid sites and cracking over Brönsted acid sites. The decrease in activity for cobalt and zinc exchanged systems can be traced to decrease in α-methyl styrene selectivity. Hence, decrease in the number of acid sites is mainly due to decrease in the number of Lewis acid sites. The low activity of Zn/Fe PM can be attributed to the higher amount of exchanged zinc as suggested by EDX and surface area measurements. NMR spectroscopy evidences the exchanged metal to be present inside the porous network thus reducing the accessibility to Lewis acid sites, which are resident mainly in the pillars.

Table 4
Catalytic activity of various systems towards cumene cracking

Catalyst	Conversion (%)	Selectivity (%)		
		α-Methyl styrene	Dealkylation products[a]	Lewis/ Brönsted[b]
V/Fe PM	29.8	53.2	46.8	1.2
Mn/Fe PM	30.2	58.9	41.1	1.4
Co/Fe PM	21.8	59.7	40.3	1.5
Ni/Fe PM	31.7	64.7	35.3	1.8
Cu/Fe PM	28.9	60.0	40.0	1.5
Zn/Fe PM	24.5	48.2	51.8	1.0
Fe PM	25.6	58.3	42.7	1.2
V/FeAl PM	22.8	54.3	45.7	1.1
Mn/FeAl PM	22.5	53.2	46.8	1.2
Co/FeAl PM	32.5	54.2	45.8	1.5
Ni/FeAl PM	28.9	60.7	39.3	1.0
Cu/FeAl PM	19.5	50.2	49.8	1.1
Zn/FeAl PM	21.1	53.3	46.7	1.7
FeAl PM	20.7	62.7	36.3	–

Reaction conditions: catalyst: 0.5 g, temperature: 400 °C, WHSV: 7 h^{-1}, time on stream: 2 h.
[a] Benzene, toluene, ethyl benzene.
[b] Ratio of α-methyl styrene and dealkylated products selectivity.

3.10. Cyclohexanol decomposition

The multifunctional character of a catalyst system is manifested through the wide diversity of products obtained with a given reactant. The product selectivity exhibited by a catalyst can be related to its surface acid base and redox properties. Alcohols, being amphoteric in nature can interact with both acidic and basic sites on the catalyst surface. Cyclohexanol undergoes dehydration over acidic sites giving cyclohexene as the major product whereas a combination of acidic and basic sites is required for dehydrogenation yielding cyclohexanone. Cyclohexene on disproportionation yields benzene, cyclohexane and methylcyclopentane [19].

The exact mechanism of gas phase dehydration of cyclohexanol has been proved difficult to study. Two possible mechanistic schemes have been proposed [20,21]. One of these is similar to E2 elimination in which the catalyst provides both an acidic site to attack the hydroxyl group and a basic site to abstract a proton. The other is similar to E1 elimination in which the

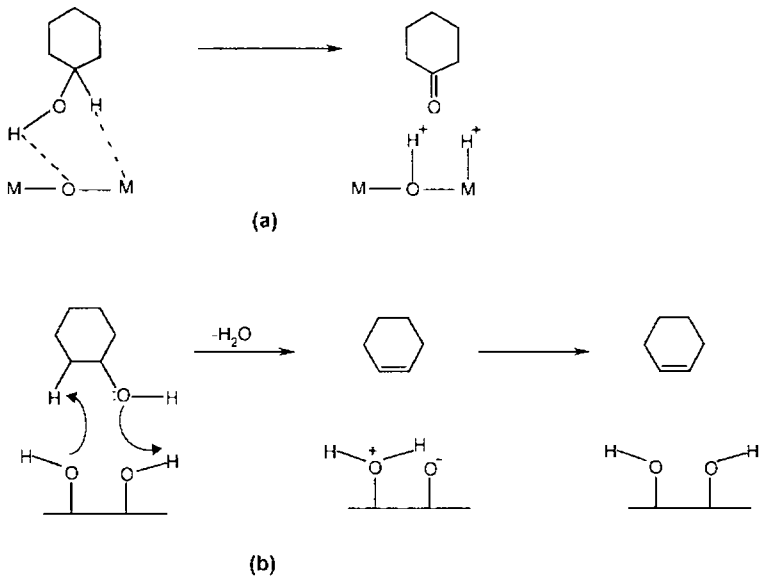

Fig. 7. Mechanism of (a) dehydrogenation and (b) dehydration of cyclohexanol on catalyst surface.

reaction proceeds through initial formation of a carbocation. Adsorption on acidic site is the rate determining step. Dehydrogenation catalysed by the acid–base sites takes place through a concerted mechanism in which the metal cation acts as Lewis acid site accepting a hydride ion while the oxygen anion acts as Brönsted base accepting the proton of the OH group. The reaction mechanism is given in Fig. 7.

The dehydration–dehydrogenation activity of cyclohexanol was tested in the vapour phase at optimised conditions. It is assumed that dehydrogenation and dehydration processes represent a set of parallel reactions obeying first order kinetics. The formation of phenol has been reported by further transformation of cyclohexanone though this was not observed in the present study. Selectivity to the product is expressed as—one selectivity (cyclohexanone) and -ene selectivity (cyclohexene). The catalytic performance of the various systems for the decomposition of cyclohexanol is presented in Table 5. Pillared clay systems show exceptional activity towards cyclohexanol decomposition. Predominant dehydration of cyclohexanol to cyclohexene occurs over the catalysts. At first sight, this fact points towards the predominantly acidic nature of catalysts and the non

Table 5
Activity of various systems towards cyclohexanol decomposition

Catalyst	Conversion (%)	Selectivity (%)			Dealkylated product selectivity (%)[d]
		Cyclohexene[a]	Cyclohexanone[b]	Others[c]	
V/Fe PM	99.0	82.9	8.9	8.2	46.8
Mn/Fe PM	91.6	85.6	9.5	4.9	41.1
Co/Fe PM	89.5	87.4	5.2	7.4	40.3
Ni/Fe PM	97.5	80.6	12.9	8.5	35.3
Cu/Fe PM	97.1	90.7	6.5	2.8	40.0
Zn/Fe PM	99.8	81.9	8.2	9.9	51.8
Fe PM	60.3	84.0	8.2	11.8	42.7
V/FeAl PM	93.5	82.0	7.0	11.0	45.7
Mn/FeAl PM	95.5	82.3	7.9	7.8	46.8
Co/FeAl PM	98.1	84.9	7.2	7.9	45.8
Ni/FeAl PM	96.7	91.5	2.1	6.4	39.3
Cu/FeAl PM	95.3	83.1	7.1	9.8	49.8
Zn/FeAl PM	97.7	81.2	8.7	11.1	46.7
FeAl PM	59.2	87.5	5.2	12.0	36.3

Reaction conditions: catalyst: 0.5 g, WHSV: 9.9 h^{-1}, temperature: 250 °C, TOS: 2 h.

[a] Formed over acidic sites.

[b] Formed by the concerted action of acidic and basic sites.

[c] Formed by the decomposition of cyclohexene.

[d] As obtained from cumene cracking reaction.

existence of sufficient basic sites. Exchange with transition metals causes a noticeable enhancement in decomposition activities of all pillared systems.

The dehydration activities of various systems run almost parallel with the amount of Brönsted acid sites as obtained from cumene cracking test reaction. The -ene selectivity for the reaction has been suggested as an index for the amount of Brönsted acidity [22]. Dehydration activity is much higher than expected from benzene selectivity values and hence cannot be explained in terms of the amount of Brönsted sites alone. For clays, it has been postulated that a Brönsted acid site upon dehydroxylation yields a Lewis acid site. Also, a Lewis acid site can be converted to a Brönsted site in presence of a water molecule [23]. Hence the effect of water formed by dehydration of cyclohexanol has to be taken into account. Conversion of Lewis acid sites to Brönsted ones can occur on clays, with the absorption of water produced on dehydration resulting in enhanced amounts of Brönsted acid sites, increasing the dehydration activity of cyclohexanol. On the other hand, dehydrogenation to cyclohexanone takes place through a concerted mechanism of Lewis acid sites and Brönsted basic sites. Increase in the Brönsted acid sites at the expense of Lewis acid sites, decreases the dehydrogenation activity of the systems. The reduced -ene selectivity can thus be attributed not only to a lower amount of basic sites but also to a decreased amount of Lewis acid sites on hydroxylation.

4. Conclusions

The various points that can be summarised from the preceding discussion are

- EDX analysis shows that increase in amount of pillared metal is at the expense of exchangeable cations. 1–3% of transition metals were incorporated on exchange.
- Surface area and pore volume measurements increases substantially upon pillaring. 60–70% of the total surface area can be attributed to micropores. Transition metal exchange decreases the surface area, especially the external surface area.
- X-ray diffraction peaks suggests shifting of 2θ values implying expansion of clay layer during pillaring process. Presence of Fe substituted Al_{13} like polymers are detected in the mixed pillared system. Insertion of the second metal after the formation of stable pillars does not destabilise the porous network.
- IR spectra of the various samples could be assigned properly. The vibrations on the framework region does not change on pillaring, indicating the structural integrity of the clay layers.
- For iron pillared systems, ^{27}Al NMR peaks are broader due to relaxation effects of the paramagnetic centres. The structure of mixed pillared systems is similar to Al polymeric species. Incorporation of transition metals does not affect the structural stability of the layers and pillars.
- ^{29}Si NMR spectra reveal that majority of the silicon tetrahedra is linked to 3 Si atoms and one Al atom. The distribution of silicon tetrahedra into various environments is not affected by pillaring. The strain in local environment of the Si atoms, is proportional to the size of intercalated species.
- The pillared clays possess substantial thermal stability. Dehydration and dehydroxylation of the clay layers occurs. The thermal stability of the pillared clays is in the order FeAl PM > Fe PM.
- UV-DRS supports the presence of the Keggin cation in mixed pillared systems. The spectrum shows a band that could be assigned to the polyoxoiron complexes.
- Surface acidity as determined by cumene cracking test reaction shows a greater percentage of Lewis acid sites on the exchanged systems.
- Cyclohexanol decomposition reaction indicated the presence of basic sites on pillared clays. Exchange with transition metals causes a noticeable enhancement in decomposition activities. On the average, dehydrogenation activities and -ene/-one selectivities are higher for iron containing systems whereas the dehydrogenation activities of aluminium pillared systems are monotonously much lower.

Acknowledgement

Financial assistance from CSIR, New Delhi to K. Manju is gratefully acknowledged.

References

[1] M.L. Occelli, Ind. Eng. Chem. Prod. Res. Dev. 22 (1983) 553–559.
[2] D.E.W. Waughan, Catal. Today 2 (1988) 178–192.
[3] F. Figueras, Catal. Rev.: Sci. Eng. 30 (3) (1988) 457–499.
[4] A. Gil, L.M. Gandia, M.A. Vicente, Catal. Rev. Sci. Eng. 42 (2000) 145–212.
[5] C.I. Warburton, Catal. Today 2 (1988) 271–280.
[6] J. Ravichandran, B. Sivasankar, Clays. Clay Miner. 45 (1997) 854–858.
[7] S.A. Zubkov, L.M. Kustov, V.B. Kazansky, G. Fetter, D. Tichit, F. Figueras, Clays. Clay Miner. 42 (1994) 421–427.
[8] M. Dobrovolsky, P. Tetenyi, Z. Paal, J. Catal. 74 (1982) 31.
[9] K. Othmer, in: F.H. Mark et al. (Eds.), Encyclopedia of Chemical Technology, Vol.7, John Wiley & Sons Inc, New York, 1979, p. 410.
[10] W.S. Chen, M.D. Lee, Appl. Catal. A 83 (1992) 201.
[11] F. Bergaya, N. Hassoun, J. Barraoult, L. Gatineau, Clay Miner. 28 (1993) 109.

[12] T. Bakas, A. Moukarika, V. Papaefthymiou, A. Ladavos, Clays. Clay Miner. 42 (1994) 634–642.
[13] D. Zhao, G. Wang, Y. Yang, X. Guo, Q. Wang, Clays. Clay Miner. 41 (1993) 317.
[14] D. Plee, F. Borg, L. Gatineau, J.J. Fripiat, J. Amer. Chem. Soc. 107 (1985) 2362–2369.
[15] L. Li, X. Liu, Y. Ge, R. Xu, J. Rocha, J. Klinowski, J. Phys. Chem. 97 (1993) 10389–10393.
[16] K.A. Karrado, A. Kostapapas, S.L. Suib, R.W. Coughlin, Solid State Ion. 22 (1986) 117–125.
[17] P. Canizares, J.L. Velverde, M.R. Sun Kou, C.B. Molina, Micropor. Mesopor. Mater. 29 (1999) 267–281.
[18] T. Sano, Y. Uno, Z.B. Zang, C.H. Ahn, K. Soga, Micropor. Mesopor. Mater. 31 (1999) 89–95.
[19] M.C.C. Costa, L.F. Hodson, R.A.W. Johnstone, J.Y. Liu, D. Whitaker, J. Mol. Catal. 142 (1999) 349.
[20] C.L. Kibby, S.S. Lande, W.K. Hall, J. Am. Chem. Soc. 94 (1972) 214.
[21] M. Ai, J. Catal. 40 (1975) 318.
[22] C.G. Ramankutty, S. Sugunan, B. Thomas, J. Mol. Catal. A: Chem. 187 (2002) 105–117.
[23] J.P. Rupert, W.T. Granquist, T.J. Pinnavia, Chemistry of Clays and Clay Minerals. A.C.D Newman (ed), 1987.